Solution Structure and Cell Selectivity of Piscidin 1 and Its Analogues[†,‡]

Sung-Ah Lee,[§] Yu Kyoung Kim,[∥] Shin Saeng Lim,[⊥] Wan Long Zhu,[⊥] Hyunsook Ko,[∥] Song Yub Shin,[⊥,#] Kyung-Soo Hahm,[⊥,#] and Yangmee Kim*[,§,∥]

Department of Bioscience and Biotechnology, Bio/Molecular Informatics Center, IBST, Konkuk University, Seoul 143-701, Korea, Department of Chemistry, Konkuk University, Seoul 143-701, Korea, Department of Bio-Materials, Graduate School and Research Center for Proteineous Materials, Chosun University, Gwangju 501-759, Korea, and Department of Cellular & Molecular Medicine, School of Medicine, Chosun University, Gwangju 501-759, Korea

Received October 27, 2006; Revised Manuscript Received January 15, 2007

ABSTRACT: Piscidin 1 (Pis-1) is a novel cytotoxic peptide with a cationic α-helical structure that was isolated from the mast cells of hybrid striped bass [Silphaduang, U., and Noga, E. J. (2001) *Nature 414*, 268−269]. Pis-1 is not selective for bacterial versus mammalian cells. In the present study, to develop novel antibiotic peptides with selectivity for bacterial cells, we examined the effect of substituting two glycine residues, Gly^8 and Gly^{13}, with Ala or Pro on this peptide's structure and biological activities. The bacterial cell selectivity of the peptides decreased in the following order: Gly→Pro analogues > Gly→Pro/Ala analogues > Pis-1 > Gly→Ala analogues. The antimicrobial and hemolytic activities and abilities to permeabilize the model phospholipid membranes were higher for Pis-1 with Gly or Pro at position 8 than for its counterparts with either Gly or Pro at position 13. We determined the tertiary structure of Pis-1 and its analogues in the presence of SDS micelles by NMR spectroscopy. We found that Pis-1 has an α-helical structure from Phe^2 to Thr^{21}. Also, Pis-1 AA (Gly^8, Gly^{13}→Ala^8, Ala^{13}) with higher antibacterial and hemolytic activity than Pis-1 has a stable α-helical structure from Phe^2 to Thr^{21}. Pis-1 PG (Gly→Pro^8) with bacterial cell selectivity has a hinge structure at Pro^8, which provides flexibility in piscidin, followed by a three-turn helix from Val^{10} to Gly^{22} in the C-terminal region. Taken together, our results demonstrate that the conformational flexibility provided by introduction of a Pro at position 8, coupled with the primary anchoring of phenylalanines and histidines in the N-terminus to the cell membrane and the optimal length of the C-terminal amphipathic α-helix, are the critical factors that confer antibacterial activity and bacterial cell selectivity to Pis-1 PG. Pis-1 PG may be a good candidate for the development of a new drug with potent antibacterial activity but without cytotoxicity.

Antimicrobial peptides have been isolated from a wide range of animal, plant, and bacterial species. Antimicrobial peptides are known to play important roles in the host defense system and innate immunity of all species (*1*−*4*). There has been enormous interest in these peptides as a new class of antibiotics with potential clinical value in the fight against multi-drug resistant microorganisms. The antimicrobial activities of these peptides are related to their abilities to adopt an amphipathic structure including an α-helix, *β*-sheet, or *β*-turn. The antibiotic action appears to involve depolarization or permeabilization of the bacterial cell membrane, although the detailed mechanisms have not been fully elucidated (*5*−*8*).

Piscidin is the first antimicrobial amphipatic cationic peptide family isolated from fish, where it is produced by mast cells, which are immune cells of uncertain function present in all vertebrates. Piscidin was isolated from the tissues of hybrid striped bass (*Morone saxatilis x M. chrysops*), an important aquaculture fish (*9*−*11*). Piscidin plays important roles in the natural innate immune system of fish, and of all piscidin peptides, piscidin 1 (Pis-1) has the highest antibacterial activity (*9*−*11*). Pis-1 is a 22-amino acid peptide with a highly conserved amino-terminus rich in histidine and phenylalanine. Recently, solid-state nuclear magnetic resonance (NMR) measurements were used to show that Pis-1 adopts an amphipathic α-helical conformation with hydrophilic and hydrophobic residues on opposing sides, similar to many other linear antimicrobial peptides (*12*). Pis-1 has potent activity against a wide variety of microbes, namely, filamentous fungi, yeast, and Gram-positive and -negative bacteria including antibiotic-resistant bacteria; however, this peptide causes hemolysis and is cytotoxic,

[†] This work was supported by a Molecular and Cellular BioDiscovery Research Program grant (M10301030001-05N0103-00110) from the Ministry of Science and Technology, and by an ERC grant from the Ministry of Science and Technology, Korea, and the Korea Science and Engineering Foundation through the Research Center for Proteineous Materials (R11-2000-083-00000-0). S.-A.L. is supported, in part, by the second BK21 (MOE).

[‡] The atomic coordinates for 20 final structures have been deposited with the Protein Data Bank under the file names 2OJM, 2OJO, and 2OJN.

* Corresponding author: Department of Bioscience and Biotechnology, Konkuk University, 1 Hwayang-dong, Kwangjin-gu, Seoul 143-701, Korea. Tel: 822-450-3421. Fax: 822-3436-5382. E-mail: ymkim@konkuk.ac.kr.

[§] Department of Bioscience and Biotechnology, Bio/Molecular Informatics Center, IBST, Konkuk University.

[∥] Department of Chemistry, Konkuk University.

[⊥] Department of Bio-Materials, Graduate School and Research Center for Proteineous Materials, Chosun University.

[#] Department of Cellular & Molecular Medicine, School of Medicine, Chosun University.

10.1021/bi062233u CCC: $37.00
Published on Web 03/01/2007

which may limit its therapeutic use (*9*−*13*). Therefore, it is very important to design new antibiotic peptides based on piscidin that are not cytotoxic.

Although Pro is commonly known as a helix-breaking amino acid, it has been found in the putative transmembrane helices of integral membrane proteins (*14*, *15*). It has been proposed that Pro in the membrane-spanning helices facilitates gating by the channel (*14*). Also, a number of α-helical antimicrobial peptides that display membrane-penetrating activity, such as melittin, caerin 1.1, buforin, gaegurin, and alamethicin, contain Pro residues in their central portion (*16*−*20*). In many antimicrobial peptides, a Pro residue disturbs the hydrogen bond patterns in the middle of the helix, leading to helix−hinge−helix structures that provide flexibilities to the peptide and increase bacterial cell selectivities (*21*, *22*). For example, introducing proline residues in the linear α-helical antimicrobial peptide in IsCT, which is a non-cell-selective antimicrobial peptide isolated from the scorpion *Opisthacanthus madagascariensis*, caused a proline-induced bend structure and the drastic decrease of the cytotoxicity of the peptide (*22*). Therefore, introducing proline residues in the α-helical antimicrobial peptide can be a good strategy to increase the bacterial cell selectivity.

Here, we investigated the tertiary structure of Pis-1 and designed a new potent peptide with bacterial cell selectivity based on the structure of Pis-1. We synthesized Pis-1 and a series of Gly→Ala analogues (Pis-1 AG, Pis-1 GA, and Pis-1 AA), Gly→Pro analogues (Pis-1 PG, Pis-1 GP, and Pis-1 PP), and Gly→Ala/Pro analogues (Pis-1 AP and Pis-1 PA). We then evaluated their toxicity to bacteria and human erythrocytes as well as their abilities to permeabilize the model phospholipid membranes.

Furthermore, to elucidate the structure−activity relationship of the peptides, we examined the tertiary structures of Pis-1 and its analogues in membrane-mimicking environments. Interactions between these peptides and the membrane were also studied by circular dichroism (CD[1]), NMR spectroscopy, and fluorescence spectroscopy. Structure−antibiotic activity relationships of these peptides should help understand their selectivities for bacterial cell membranes and therefore aid in the design of potent bacterial-selective antimicrobial peptides.

EXPERIMENTAL PROCEDURES

Peptide Synthesis. All peptides specified in Tables 1 and 2 were prepared by solid-phase synthesis using Fmoc chemistry. Peptides were purified by reversed-phase preparative high-performance liquid chromatography on a C_{18} column (20 × 250 mm; Shim-pack) using a gradient of 20% to 50% acetonitrile in H_2O with 0.1% TFA delivered over 30 min. Analytical high-performance liquid chromatography with an ODS column (4.6 × 250 mm; Shim-pack) revealed that purified peptides were more than 95% homogeneous (data not shown). The peptides also had the correct atomic masses as determined by matrix-assisted laser desorption/ionization time-of-flight mass spectrometry (Table 1).

Table 1: Amino Acid Sequences and Mass Spectral Data for Pis-1 and Its Analogues

peptide	amino acid sequence[a]	molecular mass (Da) calcd MS	molecular mass (Da) measd MS
Pis-1 (native)	FFHHIFRGIVHVGKTIHRLVTG	2572.1	2572.3
Pis-1 AG	FFHHIFR**A**IVHVGKTIHRLVTG	2586.1	2586.9
Pis-1 GA	FFHHIFRGIVHV**A**KTIHRLVTG	2586.1	2586.3
Pis-1 AA	FFHHIFR**A**IVHV**A**KTIHRLVTG	2600.1	2600.0
Pis-1 PG	FFHHIFR**P**IVHVGKTIHRLVTG	2612.1	2612.1
Pis-1 GP	FFHHIFRGIVHV**P**KTIHRLVTG	2612.1	2611.2
Pis-1 PP	FFHHIFR**P**IVHV**P**KTIHRLVTG	2652.2	2651.5
Pis-1 AP	FFHHIFR**A**IVHV**P**KTIHRLVTG	2626.1	2626.2
Pis-1 PA	FFHHIFR**P**IVHV**A**KTIHRLVTG	2626.1	2627.0
Pis-1 aa	FFHHIFR**a**IVHV**a**KTIHRLVTG	2600.1	2600.8
Pis-1 PG-3FA	**AA**HHI**A**R**P**IVHVGKTIH-RLVTG	2383.8	2383.6
Pis-1 PG-2HA	FF**AA**IFR**P**IVHVGKTIHRLVTG	2480.0	2481.3
Pis-1 PG-2H1RA	FF**AA**IF**AP**IVHVGKTIHRLVTG	2394.9	2394.1

[a] Amino acids in bold indicate the substituted residues. **a** indicates D-Ala.

Bacterial Strains. Escherichia coli KCTC 1682, *Salmonella typhimurium* KCTC 1926, *Pseudomonas aeruginosa* KCTC 1637, *Bacillus subtilis* KCTC 3068, *Staphylococcus epidermidis* KCTC 1917, and *Staphylococcus aureus* KCTC 1621 were purchased from the Korean Collection for Type Cultures, Korea Research Institute of Bioscience & Biotechnology (Taejon, Korea).

Antibacterial Activity. Antimicrobial activities of the peptides against selected organisms, including three Gram-positive and three Gram-negative bacteria, were determined using a broth microdilution assay. Briefly, single colonies of bacteria and fungi were inoculated into LB and cultured overnight at 37 °C. An aliquot of the culture was transferred to 10 mL of fresh LB and incubated for an additional 3−5 h at 37 °C until mid-logarithmic phase. A 2-fold dilution series of peptides in 1% peptone was prepared. The serial dilutions (100 μL) were added to 100 μL of cells (2×10^6 CFU/mL) in 96-well microtiter plates and incubated at 37 °C for 16 h. The lowest concentration of peptide that completely inhibited growth was defined as the minimal inhibitory concentration (MIC). MIC values were calculated as the average from triplicate measurements in three independent assays.

Hemolytic Activity. Hemolytic activity of the peptides was tested against human red blood cells (h-RBC). Fresh h-RBCs were washed three times with phosphate-buffered saline PBS (PBS; 35 mM phosphate buffer containing 150 mM NaCl, pH 7.4) by centrifugation for 10 min at 1000*g* and resuspended in PBS. The peptide solutions were then added to 50 μL of h-RBC in PBS to give a final volume of 100 μL and a final erythrocyte concentration of 4%, v/v. The resulting suspension was incubated with agitation for 1 h at 37 °C. The samples were centrifuged at 1000*g* for 5 min. Release of hemoglobin was monitored by measuring the absorbance of the supernatant at 405 nm. Controls for no hemolysis (blank) and 100% hemolysis consisted of human red blood cells suspended in PBS and 0.1% Triton-X 100,

[1] Abbreviations: CD, circular dichroism; $DiSC_3(5)$, 3,3′-dipropylthiodicarbocyanine iodide; DQF-COSY, double-quantum-filtered correlation spectroscopy; EYPC, egg yolk L-α-phosphatidylcholine; EYPG, egg yolk L-α-phosphatidylglycerol; h-RBCs, human red blood cells; LUV, large unilamellar vesicle; MIC, minimum inhibitory concentration; NMR, nuclear magnetic resonance; NOE, nuclear Overhauser effect; NOESY, nuclear Overhauser effect spectroscopy; SDS, sodium dodecyl sulfate; TOCSY, total correlation spectroscopy.

Table 2: Antimicrobial Activity of Pis-1 and its Analogues

	MIC: μM					
peptide	*E. coli*	*P. aeruginosa*	*S. typhimurium*	*B. subtilis*	*S. epidermidis*	*S. aureus*
Pis-1 (native)	2	4	2	2	2	4
Pis-1 AG	2	4	1	2	1	2
Pis-1 GA	2	4	0.5	0.5	0.5	2
Pis-1 AA	2	4	0.5	0.5	0.5	2
Pis-1 PG	4	4	2	2	2	8
Pis-1 GP	8	8	2	4	4	16
Pis-1 PP	16	16	8	4	16	16
Pis-1 AP	8	4	4	4	4	2
Pis-1 PA	2	4	2	2	2	2
Pis-1 aa	1	2	0.5	2	0.5	1
Pis-1 PG-3FA	16	64	32	8	16	64
Pis-1 PG-2HA	16	16	16	2	16	8
Pis-1 PG-2H1RA	>64	>64	>64	8	64	64

respectively. The percent hemolysis was calculated using the following equation:

$$\text{hemolysis (\%)} = [(\text{OD}_{405\text{ nm}}\text{ sample} - \text{OD}_{405\text{ nm}}\text{ zero lysis})/(\text{OD}_{405\text{ nm}}\text{ 100\% lysis} - \text{OD}_{405\text{ nm}}\text{ zero lysis})] \times 100$$

Calcein Leakage Assay. Calcein-entrapped LUVs composed of EYPC/EYPG (1:1, w/w) and EYPC were prepared by vortexing the dried lipid in dye buffer solution (70 mM calcein, 10 mM Tris, 150 mM NaCl, 0.1 mM EDTA, pH 7.4) (*23*). The suspension was frozen−thawed in liquid nitrogen for ten cycles and extruded through polycarbonate filters (two stacked 100 nm pore size filters) by a LiposoFast extruder (Avestin, Inc., Canada). Untrapped calcein was removed by gel filtration on a Sephadex G-50 column. Usually lipid vesicles are diluted to approximately 10-fold after passing through a Sephadex G-50 column. The eluted calcein-entrapped vesicles were diluted further to the desired final lipid concentration for the experiment. The leakage of calcein from the LUVs was monitored by measuring fluorescence intensity at an excitation wavelength of 490 nm and an emission wavelength of 520 nm on a model RF-5301PC spectrophotometer (Shimadzu, Kyoto, Japan). For determination of 100% dye-release, 10% Triton-X_{100} in Tris-buffer (20 μL) was added to dissolve the vesicles. The percentage of dye-leakage caused by the peptides was calculated as follows:

$$\text{dye-leakage (\%)} = 100 \times (F - F_0)/(F_t - F_0)$$

where F is the fluorescence intensity achieved by the peptides and F_0 and F_t are fluorescence intensities without the peptides and with Triton X-100, respectively.

CD Analysis. CD experiments were performed using a J-810 spectropolarimeter (Jasco, Tokyo, Japan) with a 1 mm path length cell. The CD spectra of the peptides at 100 μM were recorded at 25 °C in 0.1 nm intervals from 190 to 250 nm. To investigate the conformational changes induced by membrane environments, 2,2,2-trifluoroethanol (TFE)/water solution, dodecylphosphocholine (DPC) micelles, and sodium dodecyl sulfate (SDS) micelles of defined composition were added to the peptides. For each spectrum, the data from 10 scans was averaged and smoothed using J-810. CD data were expressed as the mean residue ellipticity $[\theta]$ in deg cm^2 dmol^{-1}. The percentage of α-helical structure was calculated as follows:

$$\%\ \alpha\text{-helical content} = ([\theta]_{222} - [\theta]^0_{222})/([\theta]^{100}_{222} - [\theta]^0_{222}) \times 100$$

where $[\theta]_{222}$ is the experimentally observed mean residue ellipticity at 222 nm, and values for $[\theta]^0_{222}$ and $[\theta]^{100}_{222}$, which correspond to 0% and 100% helix content at 222 nm, are estimated to be −2000 and −32 000, respectively (*24*).

NMR Experiments. Perdeuterated SDS was purchased from Cambridge Isotope Laboratories (Andover, MA). Peptides were dissolved at 1.5 mM in 0.45 mL of 9:1 (v/v) H_2O/D_2O (pH 4.12) containing 300 mM SDS micelles. At 318 K and 300 mM SDS micelles, the best NMR spectra were obtained. Phase-sensitive two-dimensional experiments, including double-quantum-filtered correlation spectroscopy (DQF-COSY), total correlation spectroscopy (TOCSY), and nuclear Overhauser effect spectroscopy (NOESY), were performed by time-proportional phase incrementation (*25*−*28*). For TOCSY and NOESY experiments, 450 to 512 transients with 2 K complex data points were collected for each increment with a relaxation delay of 1.2 s between the successive transients, and the data along the t_1 dimension were zerofilled to 1 K before two-dimensional Fourier transformation. TOCSY experiments were performed using 50 and 80 ms MLEV-17 spin-lock mixing pulses. Mixing times of 150, 250, and 350 ms were used for NOESY experiments. For DQF-COSY experiments, 512 transients with 4 K complex data points were collected for each increment, and the data along the t_1 dimension were zerofilled to 4 K before two-dimensional Fourier transformation. The $^3J_{HN\alpha}$ coupling constants were measured from the DQF-COSY spectra with a spectral width of 4194.631 Hz and a digital resolution of 1.02 Hz/point. Chemical shifts are expressed relative to the 4,4-dimethyl-4-silapentane-1-sulfonate signal at 0 ppm. To investigate the intramolecular hydrogen bonding in the peptides, temperature coefficients were calculated from the TOCSY experiments at 303, 313, 318, and 323 K. All of the NMR spectra were recorded on a Bruker 400 MHz spectrometer at Konkuk University and a 600 MHz spectrometer at Korea Basic Science Institute. NMR spectra were processed with NMRPipe (*29*) and visualized with Sparky (*30*).

Structure Calculations. Distance constraints were extracted from the NOESY spectra with mixing times of 150 and 250

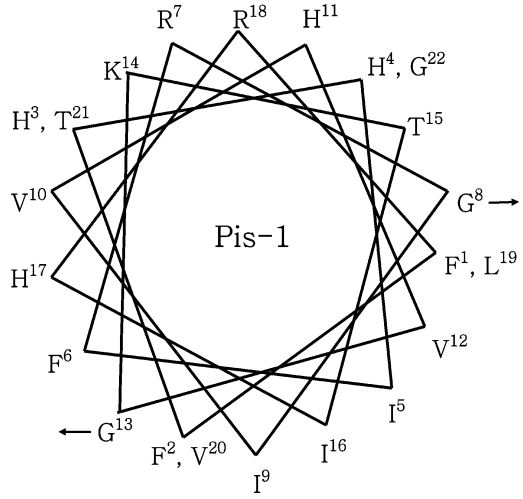

FIGURE 1: The α-helical wheel diagram of Pis-1. The arrows indicate the positions of amino acid substitutions in Pis-1. The Pis-1 wheel is amphipathic with the hydrophobic residues in the lower part and the hydrophilic residues in the upper part.

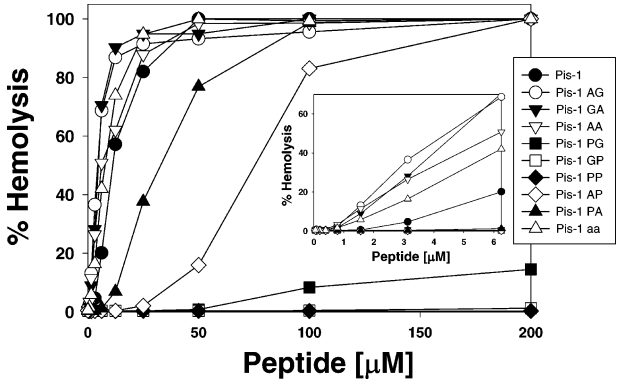

FIGURE 2: Dose−response of hemolytic activity of the peptides against h-RBCs.

ms. The volumes of the nuclear Overhauser effects (NOEs) between the two beta protons of the Phe residue were used as references. All other volumes were converted into distances by assuming a $1/r^6$ distance dependence. All of the NOE intensities were divided into three classes depending on their distance ranges: strong, 1.8 to 2.7 Å; medium, 1.8 to 3.5 Å; and weak, 1.8 to 5.0 Å (*31*, *32*). Structure calculations were carried out using XPLOR version 3.851 with the topology and parameter sets topallhdg and parallhdg, respectively. Standard pseudoatom corrections were applied to the non-stereospecifically assigned restraints (*33*), and an additional 0.5 Å was added to the upper bounds for NOEs involving methyl protons (*34*). A hybrid distance geometry-dynamical simulated annealing protocol (*35*, *36*) was employed to generate the structures. The target function that is minimized during simulated annealing comprises only quadratic harmonic potential terms for covalent geometry, square-well quadratic potentials for the experimental distance and torsion angle restraints, and a quartic van der Waals repulsion term for the nonbonded contacts. The target function did not contain hydrogen bonding, electrostatic, or 6-12 Lennard-Jones empirical potential energy terms. A total of 50 structures were generated, and the 20 structures with the lowest energies were selected for further analysis.

RESULTS

Antimicrobial and Hemolytic Activity of the Peptides. In order to design a new potent peptide with bacterial cell selectivity based on the structure of Pis-1, Pis-1 and its series of Gly→Ala analogues, Gly→Pro analogues, and Gly→Ala/Pro analogues were synthesized as listed in Table 1. The helical wheel diagram of Pis-1 in Figure 1 shows amphipathicity of Pis-1 with the hydrophobic residues in the lower region and the hydrophilic residues in the upper region. As shown in Figure 1, Gly^8 is located at the boundary of the hydrophobic and hydrophilic phases of the amphipathic α-helix, whereas Gly^{13} is in the middle of the hydrophobic phase. We examined the antimicrobial activities of the peptides against a representative set of bacterial strains including three Gram-negative (*E. coli*, *S. typhimurium*, and *P. aeruginosa*) and three Gram-positive species (*B. subtilis*, *S. epidermidis*, and *S. aureus*). The MIC values are shown in Table 2. Substitution of Gly with Ala increased the hydrophobicity in Pis-1 analogues. Gly→Ala analogues (Pis-1 AG, Pis-1 GA, and Pis-1 AA) displayed similar activities against Gram-negative bacteria but 2- to 4-fold higher activity against Gram-positive bacteria than Pis-1. Among Gly→Pro analogues, both Pis-1 GP and Pis-1 PP showed a 2- to 4-fold decrease in antibacterial activity relative to Pis-1. In contrast, the activity Pis-1 PG was comparable to that of Pis-1. Of Gly→Ala/Pro analogues, Pis-1 PA had the same activity as Pis-1, whereas Pis-1 AP was less active than Pis-1. As listed in Table 2, the

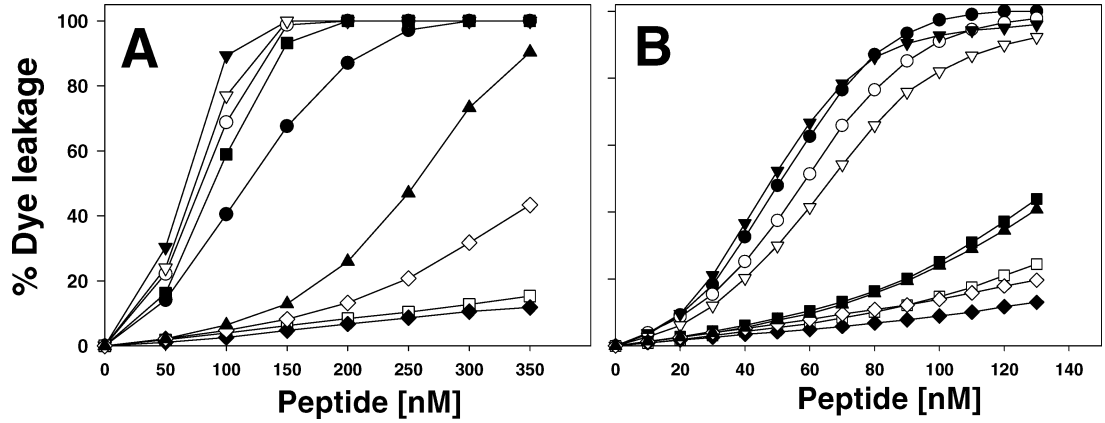

FIGURE 3: Dose−response curves of calcein-leakage from EYPC/EYPG (1:1, w/w) LUVs (A) and EYPC LUVs (B) induced by the peptides. Calcein-leakage was measured 2 min after adding the peptide. Peptides are indicated as follows: Pis-1 (●), Pis-1 AG (○), Pis-1 GA (▼), Pis-1 AA (▽), Pis-1 PG (■), Pis-1 GP (□), Pis-1 PP (◆), Pis-1 AP (◇), Pis-PA (▲).

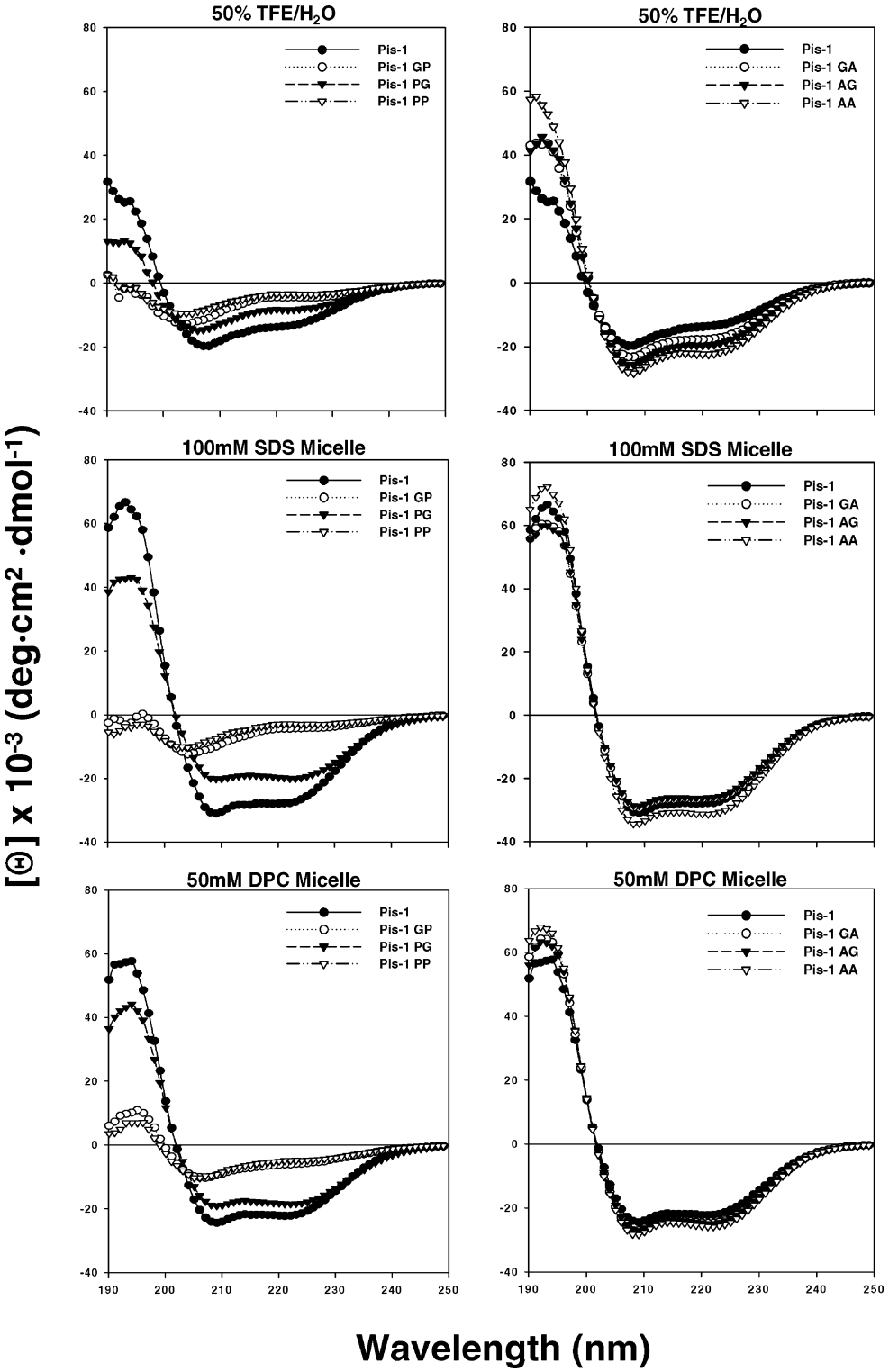

FIGURE 4: CD spectra of Pis-1 and its analogues in 50% TFE/water solution, in 100 mM SDS micelles, and in 50 mM DPC micelles. In the left side, CD spectra of Pro series peptides are shown. In the right side, CD spectra of Ala series peptides are shown.

antimicrobial activity of the peptides decreased in the following order: Pis-1 AA = Pis-1 GA > Pis-1 AG > Pis-1 = Pis-1 PA > Pis-1 PG > Pis-1 GP ≫ Pis-1 PP.

In order to investigate the effect of phenylalanines and histidines which are the highly conserved rich amino acids in the N-terminus of Pis-1 PG, we synthesized three analogues. Pis-1 PG-3FA has substitutions of three phenylalanines in the N-terminus with alanines, and Pis-1 PG-2HA has substitutions of two histidines in the N-terminus with alanines. As listed in Table 2, Pis-1 PG-3FA and Pis-1 PG-2HA showed much lower antibacterial activities compared to Pis-1 and Pis-1 PG. Furthermore, Pis-1 PG-2H1RA which has substitutions of two histidines and one arginine in the N-terminus of Pis-1 PG with alanines showed dramatic reduction of antibacterial activities compared to Pis-1 PG. This implies that positively charged residues such as His and Arg in the N-terminus play important roles in electrostatic interactions with negatively charged bacterial cell membrane.

Table 3: Percent α-Helical Contents of the Peptides in 50% TFE/H_2O, 100 mM SDS Micelles, or 50 mM DPC Micelles

peptide	50% TFE/H_2O	100 mM SDS micelles	50 mM DPC micelles
Pis-1 (native)	40.0	87.7	69.0
Pis-1 AG	59.9	82.0	75.3
Pis-1 GA	53.3	83.3	74.8
Pis-1 AA	69.3	99.0	88.9
Pis-1 PG	23.3	62.0	57.0
Pis-1 GP	10.4	9.6	15.4
Pis-1 PP	6.6	4.8	11.4

Also, insertion of the bulky side chains of Phe into the membrane may play important roles in its antibacterial activities.

We next checked the cytotoxicity of the peptides against mammalian cells by measuring their abilities to cause the lysis of human erythrocytes. Dose−response curves for the hemolytic activity of the peptides are shown in Figure 2. Gly→Ala analogues (Pis-1 AG, Pis-1 GA, and Pis-1 AA) had similar hemolytic activities as Pis-1, Gly→Ala/Pro analogues (Pis-1 AP and Pis-1 PA) had intermediate hemolytic activities, and Gly→Pro analogues (Pis-1 PG, Pis-1 GP, and Pis-1 PP) had the lowest hemolytic activities.

In order to investigate the effect of introduction of D-amino acid in Pis-1 on its activities, we synthesized Pis-1 aa which has D-ala at the position of Gly^8 and Gly^{13}. Pis-1 aa showed higher hemolytic activities as well as higher antibacterial activities compared to Pis-1.

Peptide-Induced Permeabilization of Lipid Vesicles. To investigate the membrane-permeabilizing ability of the peptides, we measured the release of the fluorescent marker calcein from liposomes of different compositions. We employed zwitterionic LUVs composed of EYPC, a phospholipid used for mimicking the major components of the outer leaflet of human erythrocytes, and negatively charged LUVs composed of 1:1 (w/w/) EYPC/EYPG to mimic bacterial cells. The percentage of calcein leakage 3 min after exposure to the peptide was used to assess the ability to permeabilize the membrane. Figure 3 shows the dose−response of the peptide-induced calcein release. Gly→Ala analogues were more effective at permeabilizing both zwitterionic and negatively charged vesicles than Pis-1. In contrast, both Gly→Pro analogues and Gly→Pro/Ala analogues were less potent at permeabilizing membranes than Pis-1. The relative abilities of the peptides to induce leakage from zwitterionic vesicles agrees with their relative hemolytic activities. Pis-1 PG is as effective at permeabilizing negatively charged vesicles as Pis-1, whereas it is much less effective at permeabilizing zwitterionic vesicles than Pis-1.

CD Measurement of Pis-1 and Its Analogues. We investigated the secondary structure of Pis-1 and its analogues in membrane-like environments by analyzing the CD spectra of these peptides dissolved in various kinds of membrane mimetic environments as shown in Figure 4. Pis-1 and its analogues have random structures in aqueous solution, but they have conformational changes and form α-helical conformations in 50% TFE/water solution, SDS micelles, and DPC micelles. Contents of helicity of the peptides in different membrane mimetic environments were calculated and listed in Table 3 (*24*). Pis-1 Ala series had much higher α-helicity than Pis-1, whereas the Pis-1 Pro series had a lower

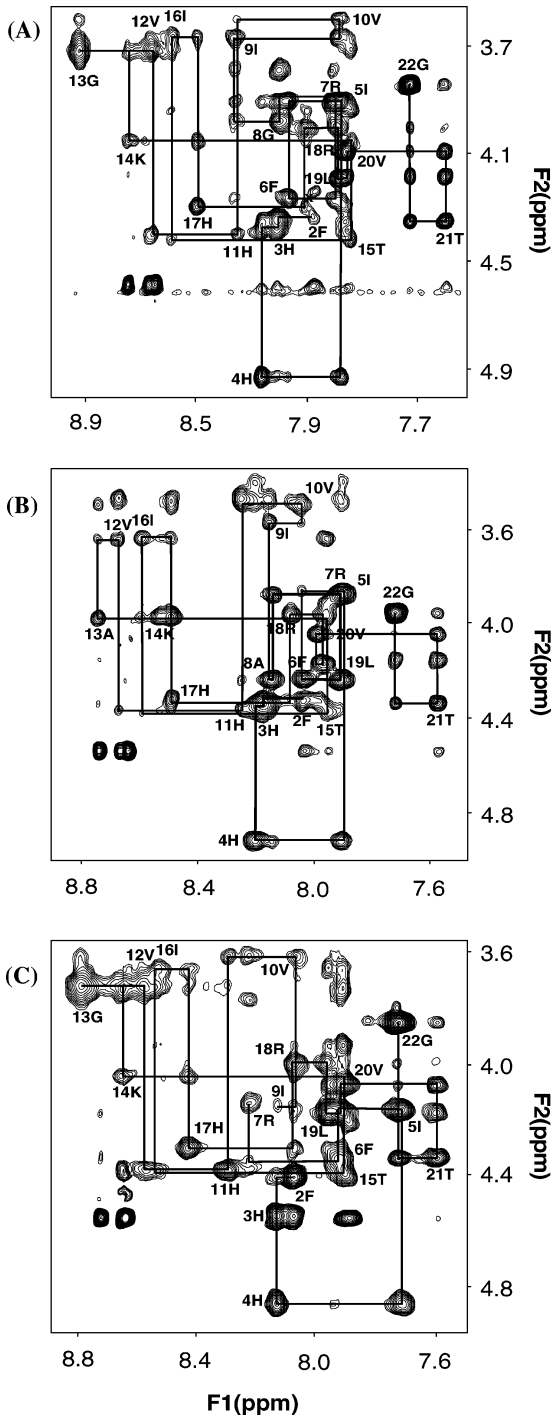

FIGURE 5: NH−C_αH region NOESY spectra of (A) Pis-1, (B) Pis-1 AA, and (C) Pis-1 PG in 300 mM SDS micelles at 318 K with a 250 ms mixing time. For clarity, only the intraresidual NH−CαH cross peaks are labeled.

α-helicity than Pis-1. Overall, the α-helicity of the Pis-1 Pro series decreased in the following order: Pis-1 > Pis-1 PG > Pis-1 GP > Pis-1 PP.

Resonance Assignment and Structure of Pis-1 and Its Analogues. We made sequence-specific resonance assignments using mainly the DQF-COSY, TOCSY, and NOESY data (*37*). Figure 5 shows the NOESY spectra with the sequential assignments for Pis-1 and its analogues in the NH−C_αH region. The chemical shifts of Pis-1, Pis-1 AA, and Pis-1 PG in 300 mM SDS micelles at 318 K, referenced to 4,4-dimethyl-4-silapentane-1-sulfonate, are listed in the

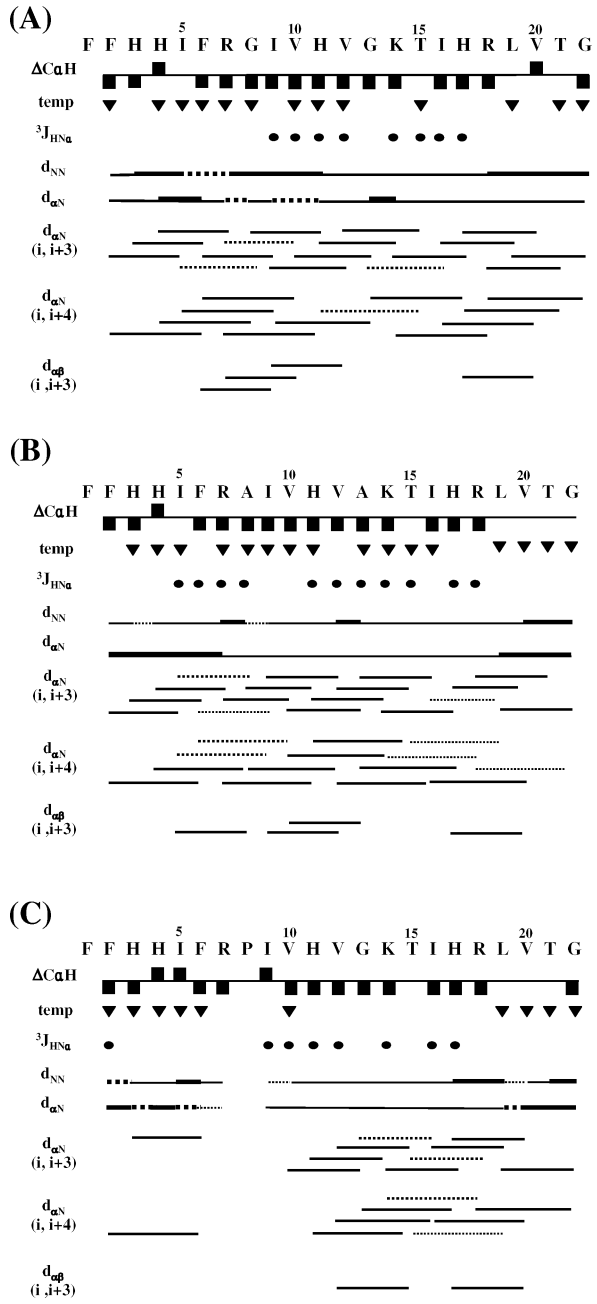

FIGURE 6: Summary of the NOE connectivities, the $^3J_{HN\alpha}$ coupling constants (●: $J_{HN} < 6$ Hz), temperature coefficients, and the CαH chemical shift index for (A) Pis-1, (B) Pis-1 AA, and (C) Pis-1 PG in 300 mM SDS micelles. The thickness of the line for the NOEs reflects the intensity of the NOE connectivities.

Supporting Information. The overall chemical shift of Pis-1 is similar to those of its analogues, with the exception of the resonances in the regions containing substitutions.

The sequential NOE connectivities and the other NMR data are illustrated in Figure 6. As shown in Figures 5 and 6, a number of nonsequential NOE connectivities that are characteristic of an α-helix, specifically $d_{\alpha N}(i,i+3)$ and $d_{\alpha N}(i,i+4)$, were observed for all of the peptides. Pis-1 and Pis-1 AA have $d_{\alpha N}(i,i+3)$ and $d_{\alpha N}(i,i+4)$ connectivities from Phe[2] to Gly[22] while Pis-1 PG has $d_{\alpha N}(i,i+3)$ and $d_{\alpha N}(i,i+4)$ connectivities from Val[10] to Gly[22]. The amide proton temperature coefficient has been used to predict hydrogen bond donors, and values above −4.5 ppb/K indicate that the amide proton is involved in intramolecular hydrogen bonding (*38*). The observed values of the $^3J_{HN\alpha}$ coupling constants for the helical region of all of the peptides were generally below 6 Hz, and temperature coefficients of the amide protons in the α-helical region of the peptides were generally above −4.5 ppb/K, indicating that Pis-1 and Pis-1 AA form stable α-helices. The ^{1}H chemical shift deviation was referenced according to the method of Wishart et al. (*39*). In the case of Pis-1 and Pis-1 AA, most of the residues have a negative ^{1}Hα chemical shift index (CSI), which implies that they have stable α-helix structures.

To calculate the tertiary structures of Pis-1 and its analogues, we used experimental restraints such as sequential ($|i - j| = 1$), medium-range ($1 < |i - j| \leq 5$), long-range ($|i - j| > 5$), intraresidual distance, hydrogen-bonding restraints, and torsion angle restraints. Of the structures that were accepted with small deviations from the idealized covalent geometry and the experimental restraints (≤0.05 Å for bonds, ≤5° for angles, ≤5° for chirality, ≤0.3 Å from NOE restraints, and ≤3° from torsion angle restraints), we analyzed 20 output structures with the lowest energy for each peptide. Figure 7 shows the superposition of the 20 lowest energy structures of Pis-1 and its analogues over the backbone atoms in 300 mM SDS micelles. None of the structures have violations over 0.5 Å from the NOE distance restraints or 3° from dihedral angle restraints, and all the structures exhibit good covalent geometry. When we superimposed the 20 lowest energy structures of Pis-1 (from Phe[2] to Thr[21]), Pis-1 AA (from Phe[2] to Thr[21]), and Pis-1 PG (from Val[10] to Gly[22]) over the backbone atoms, their root mean squared deviations from the mean structures were 0.486 ± 0.14, 0.479 ± 0.16, and 0.422 ± 0.11 Å for the backbone atoms (N, Cα, C′, O) and 1.006 ± 0.13, 1.159 ± 0.19, and 0.892 ± 0.16 Å for all heavy atoms, respectively (Table 4).

According to Procheck analysis Pis-1 has an α-helix from Phe[2] to Thr[21], as shown in Figure 8 and Figure 9A. Pis-1 AA has a stable linear amphipathic α-helical structure from Phe[2] to Thr[21], too (Figure 9B). Because of the increase in hydrophobicity caused by substitution of alanines for glycines at the 8 and 13 positions, Pis-1 AA has the largest hydrophobic area in its amphipathic α-helix and the highest antibacterial and hemolytic activities among all peptides.

As shown in Figure 9C, Pis-1 PG has a flexible bent structure at Pro[8], a short helix from Phe[2] to Phe[6], and a longer helix from Val[10] to Gly[22]. These results indicate that proline forms a flexible hinge and that this hinge at the central region of a helical antimicrobial peptide is important for conferring high selectivity against bacterial cells. Pis-1 GP and Pis-1 PP showed a few inter-residual NOEs because they have much more flexible structures than Pis-1, Pis-1 AA, and Pis-1 PG.

DISCUSSION AND CONCLUSION

To investigate the structure−activity relationship of piscidin and to design novel peptide antibiotics with selectivity for bacterial cells, we evaluated how its structure, antibacterial/hemolytic activity, and interaction with phospholipid membranes are affected by substituting the glycine at positions 8 or 13 with alanine or proline. To develop antibiotic drugs with therapeutic potential, the peptide must be toxic to bacterial cells but not significantly toxic to mammalian cells. Table 5 lists the peptide concentration

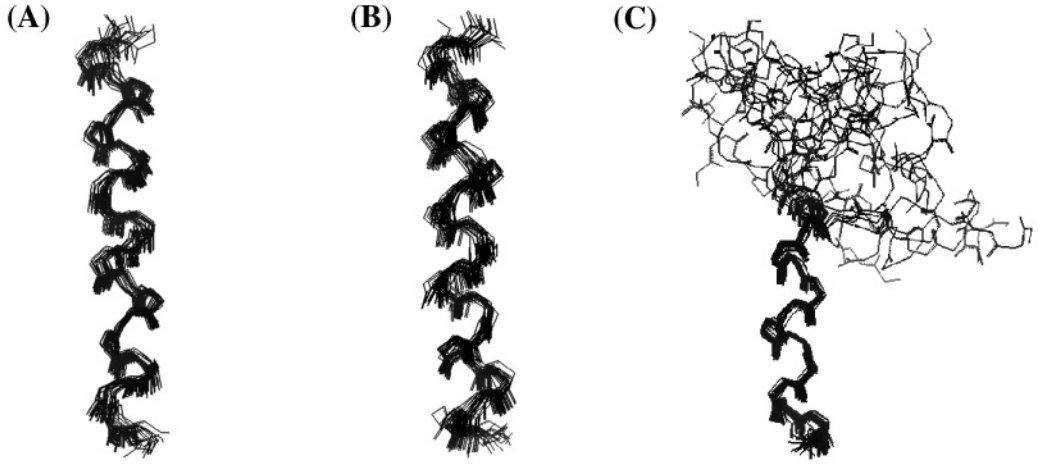

FIGURE 7: The superpositions of the 20 lowest energy structures calculated from the NMR data for (A) Pis-1, (B) Pis-1 AA, and (C) Pis-1 PG in 300 mM SDS micelles. For Pis-1 and Pis-1 AA, the backbone atoms of residues 2 to 21 were superimposed. In the case of Pis-1 PG, backbone atoms of residues 10 to 22 were superimposed.

Table 4: Structural Statistics and Mean Pairwise Root Mean Squared (rmsd) Deviations for the 20 Best Structures of Pis-1 and Its Analogues in SDS Micelles at 318 K[a]

restraints for structure calculation	Pis-1	Pis-1 AA	Pis-1 PG
experiment distance restraints			
total	294	279	247
sequential	98	87	118
medium range	49	35	38
intraresidue	121	119	78
hydrogen-bond restraints	18	18	7
dihedral angle restraints	8	20	6
rmsd from experimental geometry			
NOE (Å)	0.040 ± 0.00	0.022 ± 0.00	0.032 ± 0.00
ϕ (deg)	0.397 ± 0.18	0.119 ± 0.05	0.395 ± 0.13
rmsd from covalent geometry			
bonds (Å)	0.004 ± 0.00	0.002 ± 0.00	0.003 ± 0.00
angles (deg)	0.525 ± 0.01	0.456 ± 0.01	0.533 ± 0.02
impropers (deg)	0.390 ± 0.01	0.323 ± 0.01	0.391 ± 0.01
average energies (kcal mol^{-1})			
E_{tot}	65.72 ± 1.77	34.73 ± 2.00	56.46 ± 5.66
E_{NOE}	22.77 ± 0.83	6.39 ± 1.15	11.89 ± 2.06
E_{tor}	0.09 ± 0.11	0.02 ± 0.01	0.08 ± 0.05
E_{repel}	4.09 ± 0.76	1.62 ± 0.67	6.50 ± 2.12
rmsd from the mean structure			
backbone atoms of all residues	0.553 ± 0.15	0.569 ± 0.19	2.774 ± 0.50
all heavy atoms of all residues	1.159 ± 0.16	1.280 ± 0.20	3.932 ± 0.56
backbone atoms of residues (2−21, 2−21, 10−22)	0.486 ± 0.14	0.479 ± 0.16	0.422 ± 0.11
all heavy atoms of residues (2−21, 2−21, 10−22)	1.006 ± 0.13	1.159 ± 0.19	0.892 ± 0.16

[a] E_{NOE}, E_{tor}, and E_{repel} are the energies related to the NOE violations, the torsion angle violations, and the van der Waals repulsion term, respectively. The value of the square-well NOE (E_{NOE}) and torsion angle (E_{tor}) potentials were calculated with force constants of 50 kcal mol^{-1} Å^{-2} and 200 kcal mol^{-1} rad^{-2}, respectively. The values of the quartic van der Waals repulsion term (E_{repel}) was calculated with a force constant 4 kcal mol^{-1} Å^{-4}. The rmsd values were obtained by best fitting the backbone atom (N, C, C′, and O) coordinates for all residues of the 20 converged structures. The numbers given for the backbone and all heavy atoms represent the mean values ± standard deviations.

causing 50% hemolysis of h-RBCs (HC_{50}), the average MIC value for six bacterial strains, and the relative cell selectivity index (RSI), which is the ratio of HC_{50} to the average MIC for a peptide divided by that of Pis-1. A high RSI is thus an indication of two preferred characteristics of the peptide: a high HC_{50} (low hemolysis) and a low MIC (high antimicrobial activity). Gly→Ala analogues (Pis-1 AG, Pis-1 GA, and Pis-1 AA) had lower RSIs than Pis-1, whereas Gly→Pro analogues (Pis-1 PG, Pis-1 GP, and Pis-1 PP) had much higher RSIs. Also, substitution of Gly with D-ala in Pis-1 aa increased the cytotoxicity and decreased the RSI values. Pis-1 PG had similar antibacterial activity as Pis-1 but has the highest RSI values among all the analogues.

The tertiary structure of Pis-1 in the presence of SDS micelles, which mimics the negatively charged bacterial phospholipid membrane, showed that Pis-1 contains an amphipathic α-helical structure from Phe^2 to Thr^{21}. This finding is consistent with recent solid-state NMR data (*12*). Figures 8A and 8B show the orientation of the hydrophobic and hydrophilic side chains of Pis-1. It is well-known that when an amphipathic peptide forms an ion channel, the hydrophilic residues face inward to contact the solvent and the hydrophobic side chains face toward the acyl chains of the hydrophobic lipid (*21*, *40*−*42*). The hydrophobic side chains (colored red in Figure 8) protrude toward one side, and the hydrophilic side chains (colored blue) protrude toward the other side. Analysis of the tertiary structures of the Pis-1 analogues revealed that the substitution of Gly^8 with alanine or proline greatly affects its structure, antibacterial/hemolytic activity, and interaction with phospholipid

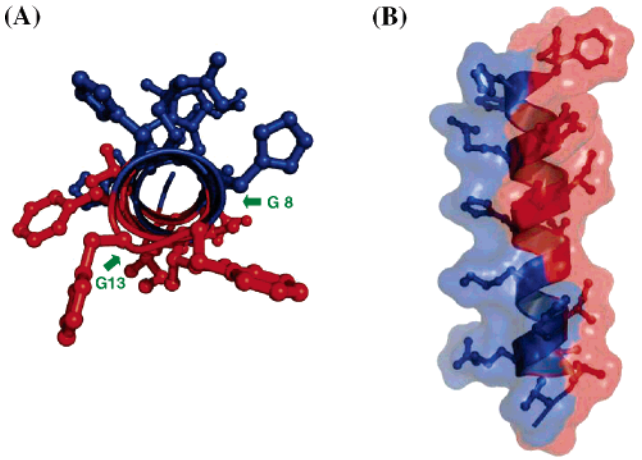

FIGURE 8: (A) Head-on view of Pis-1. The hydrophobic side chains are indicated in red, and the hydrophilic side chains are shown in blue. Gly^8 and Gly^{13} are indicated by arrows. (B) Hydrophobic surface model of Pis-1 in 300 mM SDS micelles at 318 K. The hydrophobic side chains are indicated in red, and the hydrophilic side chains are shown in blue.

membranes. Gly^{13} is in the middle of the hydrophobic phase, and substitution of Gly^{13} with Ala^{13} increases the hydrophobic area of Pis-1. Therefore, Pis-1 GA and Pis-1 AA show higher antimicrobial and hemolytic activities than Pis-1 and Pis-1 AG. Because alanine is an α-helix promoting residue and is more hydrophobic than glycine, Pis-1 AA forms a stable α-helix from Phe^2 to Thr^{21}. The hydrophobic moment, estimated using the Eisenberg equation (*43*, *44*) of Pis-1 AA, is 0.94, which is higher than that for Pis-1 (0.82). These results confer higher hemolytic and antibacterial activity to Pis-1 AA than to Pis-1. Because of the helix-disrupting nature of proline, Pis-1 PG ($Gly^8 \rightarrow Pro^8$) has a bent structure at Pro^8, and it exhibits low hemolytic activity but retains potent antibacterial activity. These results suggest that the proline-induced bent structure of Pis-1 PG at Pro^8 is an important determinant of the selectivity for bacterial cells.

Most bacterial cell-selective antimicrobial peptides bind strongly and permeate more efficiently into negatively charged phospholipid membranes, which mimic the bacterial membranes, than into zwitterionic phospholipid membranes, which are the major components of the outer leaflet of human erythrocytes (*40*, *45*). Non-cell-selective peptides bind and efficiently permeate both negatively charged and zwitterionic phospholipid membranes (*40*, *45*). Our dye leakage experiment data showed that Pis-1 PG is more effective at permeabilizing the negatively charged vesicles which mimics the bacterial membranes than the zwitterionic vesicles. This result agrees well with its low hemolytic activity of Pis-1 PG. These data prove that Pis-1 PG can be an excellent candidate lead compound for the development of novel antimicrobial agents.

According to the recent solid-state NMR study, Pis-1 has an overall α-helical structure and is oriented parallel to the membrane surface. This study also demonstrated that peptide−lipid interactions are enhanced at the water−bilayer interface for amphipathic cationic antimicrobial peptides (*11*). It is likely that Pis-1 and Pis-1 AA, which have amphipathic α-helices, lie on the surface of the bacterial membrane. Because the hydrophobic moments of Pis-1 and Pis-AA are relatively high, when the concentrations of Pis-1 and Pis-1 AA increase at the surface of the membrane, they may cause damage to both the bacterial and the mammalian cell membrane by forming pores or disintegrating the membrane.

In the case of Pis-1 PG, it is likely that the flexible hinge near Pro^8 allows for optimal orientation of both the C- and N-terminal amphiphatic α-helices of Pis-1 PG with the membrane, thus retaining the antibacterial activities. The N-terminal segment preceding the Gly^8 of Pis-1 contains three hydrophobic phenylalanines and two histidines. The phenylalanine residues are located at a very flexible region, positions 1, 2, and 6 in the N-terminus. Pis-1 PG-3FA, Pis-1 PG-2HA, and Pis-1 PG-2H1RA showed dramatic reductions of antibacterial activities compared to Pis-1 PG. Therefore, in the case of Pis-1 PG, the partial insertion of the phenylalanines of Pis-1 PG into the membrane surface and the electrostatic interactions between the positively charged histidine and arginine residues in the N-terminus of Pis-1 PG and the anionic phospholipid head groups may provide the primary anchoring to the cell membrane. The flexibility or bending potential induced by the proline residue in the middle of the peptide may then facilitate formation of the

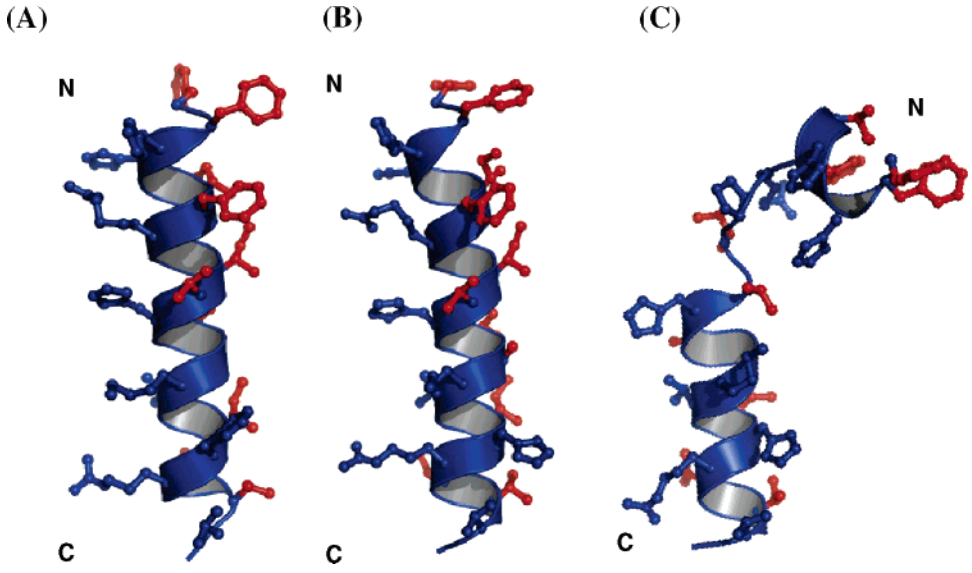

FIGURE 9: Ribbon diagram of the lowest energy structure of (A) Pis-1, (B) Pis-1 AA, and (C) Pis-1 PG in 300 mM SDS micelles.

Table 5: Relative Cell Selectivity of Pis-1 and Its Analogues

peptide	average MIC (μM)[a]	HC_{50} (μM)[b]	RSI[c]
Pis-1 (native)	2.66	11	1
Pis-1 AG	2.0	4	0.48
Pis-1 GA	1.58	4	0.61
Pis-1 AA	1.58	6	0.92
Pis-1 PG	3.66	200<	13.22<
Pis-1 GP	7.0	200<	6.91<
Pis-1 PP	12.66	200<	3.82<
Pis-1 AP	4.33	75	4.18
Pis-1 PA	2.33	32	3.31
Pis-1 aa	1.08	8	1.79

[a] Average MIC value for six bacterial strains [b] Peptide concentration causing 50% hemolysis of h-RBCs [c] Relative selectivity index: the ratio of HC_{50} to the average MIC of a given analogue divided by that for Pis-1.

C-terminal α-helix, which may penetrate the membrane, resulting in a more drastic disturbance of its structure.

Interestingly, the antimicrobial and hemolytic activities and abilities to permeabilize model membranes of Pis-1 GA, Pis-1 PG, and Pis-1 PA, which contain Gly or Pro at position 8, were higher than those of their counterparts that have Gly or Pro at position 13, namely, Pis-1 AG, Pis-1 GP, and Pis-1 AP, respectively. These results demonstrate that the flexibility of the residue at position 8, which lies at the boundary of the hydrophobic and hydrophilic phases of the amphipathic α-helix in Pis-1, plays a more important role than position 13 in enhancing antimicrobial and hemolytic activities and the ability to permeabilize membranes. Gly^{13} is located in the middle of the hydrophobic phase of the amphipathic α-helix. In the case of Pis-1 GP, replacement of Gly^{13} with Pro^{13} provides flexibility in the structure of peptides but also decreases the length of α-helix at the C-terminus. Consequently, an absence of proper interactions between the C-terminal helix and the membrane may be responsible for the inability of Pis-1 GP to interact effectively with bacterial cell membranes, reducing membrane binding and the ability to permeabilize membranes. The length of the α-helix in the C-terminus is too short to effectively penetrate the membrane so that Pis-1 GP has much lower antibacterial activity than Pis-1. Therefore, the length of the α-helix at the C-terminus, which penetrates the membrane, as well as its structural flexibility may be important determinants of antimicrobial activity and selectivity for bacterial cells.

It has been reported that diastereomers including D-amino acids exhibit better bacterial cell selectivities compared to their L-amino acid counterparts and they have a potential to be developed for therapeutic use (*46*−*48*). Also, incorporation of peptoid in various antimicrobial peptides has been proved to be a promising strategy for the rational design of intracellular, cell-selective antimicrobial peptides (*49*, *50*). As shown in this study, in case of piscidin, introduction of D-Ala (Pis-1 aa) did not reduce the toxicity of the peptide. Therefore, further studies using other strategies including introduction of peptoid in piscidin-1 which may exhibit better bacterial cell selectivities over incorporation of proline residue will be tried to develop potent peptide antibiotics. Recently, we successfully cloned and expressed Pis-1 and Pis-1 PG (*51*). In future studies, we will examine the effect of the hinge structure on the overall structure, dynamics, and mechanism of action of Pis-1 and Pis-1 PG using heteronuclear NMR spectroscopy. Understanding the structure−activity relationship of piscidin and its analogues should assist in our efforts to design novel antimicrobial peptides that have antibiotic activities with bacterial cell selectivity and no hemolytic activity.

ACKNOWLEDGMENT

We thank KBSI for providing us NMR time (NMR Research Program of Korea Basic Science Institute granted by Korean Ministry of Science & Technology).

SUPPORTING INFORMATION AVAILABLE

The chemical shifts of Pis-1, Pis-1 AA, and Pis-1 PG in the 300 mM SDS micelles at 318 K. This material is available free of charge via the Internet at http://pubs.acs.org.

REFERENCES

1. Andreu, D., and Rivas, L. (1998) Animal antimicrobial peptides: an overview, *Biopolymers 47*, 415−433.
2. Zasloff, M. (1992) Antibiotic peptides as mediators of innate immunity, *Curr. Opin. Immunol. 4*, 3−7.
3. Hancock, R. E., and Diamond, G. (2000) The role of cationic antimicrobial peptides in innate host defences, *Trends Microbiol. 8*, 402−410.
4. Shai, Y. (2002) Mode of action of membrane active antimicrobial peptides, *Biopolymers 66* (4), 236−248.
5. Epand, R. M., and Vogel, H. J. (1999) Diversity of antimicrobial peptides and their mechanisms of action, *Biochim. Biophys. Acta 1462*, 11−28.
6. Blondelle, S. E., Lohner, K., and Aguilar, M. (1999) Lipid-induced conformation and lipid-binding properties of cytolytic and antimicrobial peptides: determination and biological specificity, *Biochim. Biophys. Acta 1462*, 89−108.
7. Dathe, M., and Wieprecht, T. (1999) Structural features of helical antimicrobial peptides: their potential to modulate activity on model membranes and biological cells, *Biochim. Biophys. Acta 1462*, 71−87.
8. Hancock, R. E., and Rozek, A. (2002) Role of membranes in the activities of antimicrobial cationic peptides, *FEMS Microbiol. Lett. 206*, 143−149.
9. Silphaduang, U., and Noga, E. J. (2001) Peptide antibiotics in mast cells of fish, *Nature 414*, 268−269.
10. Noga, E. J., and Silphaduang, U. (2003) Piscidins: a novel family of peptide antibiotics from fish, *Drug News Perspect. 16*, 87−92.
11. Lauth, X., Shike, H., Burns, J. C., Westerman, M. E., Ostland, V. E., Carlberg, J. M., Van Olst, J. C., Nizet, V., Taylor, S. W., Shimizu, C., and Bulet, P. (2002) Discovery and characterization of two isoforms of moronecidin, a novel antimicrobial peptide from hybrid striped bass, *J. Biol. Chem. 277* (7), 5030−5039.
12. Chekmenev, E. Y., Vollmar, B. S., Forseth, K. T., Manion, M. N., Jones, S. M., Wagner, T. J., Endicott, R. M., Kyriss, B. P., Homem, L. M., Pate, M., He, J., Raines, J., Gor'kov, P. L., Brey, W. W., Mitchell, D. J., Auman, A. J., Ellard-Ivey, M. J., Blazyk, J., and Cotton, M. (2006) Investigating molecular recognition and biological function at interfaces using piscidins, antimicrobial peptides from fish, *Biochim. Biophys. Acta 1758* (9), 1359−1372.
13. Chinchar, V. G., Bryan, L., Silphadaung, U., Noga, E., Wade, D., and Rollins-Smith, L. (2004) Inactivation of viruses infecting ectothermic animals by amphibian and piscine antimicrobial peptides, *Virology 323* (2), 268−275.
14. Tieleman, D. P., Shrivastava, I. H., Ulmschneider, M. R., Sansom, M. S. (2001) Proline-induced hinges in transmembrane helices: possible roles in ion channel gating, *Proteins 44* (2), 63−72.
15. Li, J., Boschek, C. B., Xiong, Y., Sacksteder, C. A., Squier, T. C., and Bigelow, D. J. (2005) Essential role for Pro21 in phospholamban for optimal inhibition of the Ca-ATPase, *Biochemistry 44* (49), 16181−16191.
16. Pukala, T. L., Brinkworth, C. S., Carver, J. A., and Bowie, J. H. (2004) Investigating the importance of the flexible hinge in caerin 1.1: solution structures and activity of two synthetically modified caerin peptides, *Biochemistry 43* (4), 937−944.

17. Woolfson, D. N., Mortishire-Smith, R. J., and Williams, D. H. (1991) Conserved positioning of proline residues in membrane-spanning helices of ion-channel proteins, *Biochem. Biophys. Res. Commun. 175*, 733−737.
18. Williams, K. A., and Deber, C. M. (1991) Proline residues in transmembrane helices: structural or dynamic role?, *Biochemistry 30*, 8919−8923.
19. Park, C. B., Yi, K. S., Matsuzaki, K., Kim, M. S., and Kim, S. C. (2000) Structure-activity analysis of buforin II, a histone H2A-derived antimicrobial peptide: the proline hinge is responsible for the cell-penetrating ability of buforin II, *Proc. Natl. Acad. Sci. U.S.A. 97* (15), 8245−8250.
20. Park, J. M., Jung, J. E., and Lee, B. J. (1994) Antimicrobial peptides from the skin of a Korean frog, Rana rugosa, *Biochem. Biophys. Res. Commun. 218*, 408−413.
21. Oh, D., Shin, S. Y., Lee, S., Kang, J. H., Kim, S. D., Ryu, P. D., Hahm, K. S., and Kim, Y. (2000) Role of the hinge region and the tryptophan residue in the synthetic antimicrobial peptides, cecropin A(1-8)-magainin 2(1-12) and its analogues, on their antibiotic activities and structures, *Biochemistry 39* (39), 11855−11864.
22. Lee, K., Shin, S. Y., Kim, K., Lim, S. S., Hahm, K. S., and Kim, Y. (2004) Antibiotic activity and structural analysis of the scorpion-derived antimicrobial peptide IsCT and its analogs, *Biochem. Biophys. Res. Commun. 323* (2), 712−719.
23. Shai, Y., Bach, D., and Yanovsky, A. (1990) Channel formation properties of synthetic pardaxin and analogues, *J. Biol. Chem. 265*, 20202−20209.
24. Wu, C. S., Ikeda, K., and Yang, J. T. (1981) Ordered conformation of polypeptides and proteins in acidic dodecyl sulfate solution, *Biochemistry 20*, 566−570.
25. Derome, A., and Williamson, M. (1990) Rapid-Pulsing Artifacts in Double-Quantum-Filtered COSY, *J. Magn. Reson. 88*, 177−185.
26. Bax, A., and Davis, D. G. (1985) MLEV-17-Based Two-Dimensional Homonuclear Magnetization Transfer Spectroscopy, *J. Magn. Reson. 65*, 355−360.
27. Bax, A., and Davis, D. G. (1985) Practical Aspects of Two-Dimensional Transverse NOE spectroscopy, *J. Magn. Reson. 63*, 207−213.
28. Marion, D., and Wüthrich, K. (1983) Application of Phase Sensitive Two-Dimensional Correlated Spectroscopy (COSY) for Measurements of ^{1}H-^{1}H Spin-Spin Coupling Constants in Proteins, *Biochem. Biophys. Res. Commun. 113*, 967−974.
29. Delaglio, F., Grzesiak, S., Vuister, G., Zhu, G., Pfeifer, J., and Bax, A. (1995) NMRPipe: a multidimensional spectral processing system based on UNIX pipes, *J. Biomol. NMR 6*, 277−293.
30. Goddard, T., and Kneller, D. G. *SPARKY3*, University of California, San Francisco.
31. Clore, G. M., and Gronenborn, A. M. (1989) Determination of Three-Dimensional Structures of Proteins and Nucleic Acids in Solution by Nuclear Magnetic Resonance Spectroscopy, *CRC Crit. Rev. Biochem. Mol. Biol. 24*, 479−564.
32. Clore, G. M., and Gronenborn, A. M. (1994) Structures of Larger Proteins, Protein-Ligand and Protein-DNA Complexes by Multi-Dimensional Heteronuclear NMR, *Protein Sci. 3*, 372−390.
33. Wüthrich, K., Billeter, M., and Braun, W. (1983) Pseudostructures for the 20 Common Amino Acids for Use in Studies of Protein Conformations by Measurements of Intramolecular Proton-Proton Distance Constrains with Nuclear Magnetic Resonance, *J. Mol. Biol. 169*, 949−961.
34. Clore, G. M., Gronenborn, A. M., Nilges, M., and Ryan, C. A. (1987) Three-Dimensional Structure pf Potato carboxypeptidase inhibitor in solution: A Study Using Nuclear Magnetic Resonance, Distance Geometry, and Restrained Molecular Dynamics, *Biochemistry 26*, 8012−8023.
35. Nilges, M., Clore, G. M., and Gronenborn, A. M. (1988) Determination of Three-Dimensional Structures of Proteins from Interprotein Distance Data by Hybrid Distance Geometry-Dynamical Simulated Annealing Calculations, *FEBS Lett. 229*, 317−324.
36. Kuszewski, J., Nilges, M., and Brünger, A. T. (1992) Sampling and Efficiency of Metric Matrix Distance Geometry: A Novel Partial Metization Algorithm, *J. Biomol. NMR 2*, 33−56.
37. Wüthrich, K. (1986) *NMR of Protein and Nucleic Acid*, Wiley-Interscience, New York.
38. Baxter, N. J., and Williamson, M. P. (1997) Temperature Dependence of 1H Chemical Shifts in Proteins, *J. Biomol. NMR 9*, 359−369.
39. Wishart, D. S., Sykes, B. D., Richards, F. M. (1992) The chemical shift index: a fast and simple method for the assignment of protein secondary structure through NMR spectroscopy, *Biochemistry 31*, 1647−1651.
40. Gennis, R. B. (1989) *Biomembranes: Molecular Structure and Function*, pp 155−156, Springer-Verlag, New York.
41. Holak, T. A., Engstrom, A., Kraulis, P. J., Lindeberg, G., Bennich, H., Jones, T. A., Gronenborn, A. M. and Clore, G. M. (1988) The Solution Conformation of The Antibacterial Peptide Ccecropin A: A Nuclear Magnetic Resonance and Dynamical Simulated Annealing Study, *Biochemistry 27*, 7620−7629.
42. Katsu, T., Kuroko, M., Morikawa, T., Sanchika, K., Yamanaka, H., Shinoda, S., and Fujita, Y. (1990) Interaction of Wasp Venom Mastoparan with Biomembranes, *Biochim. Biophys. Acta 1027*, 185−190.
43. Tossi, A., Sandri, L., and Giangaspero, A. (2002) New consensus hydrophobicity scale extended to non-proteinogenic amino acids. In *Peptides 2002: Proceedings of the twenty-seventh European peptide symposium*, Edizioni Ziino, Napoli, Italy, pp 416−417.
44. Lee, K. H., Lee, D. G., Park, Y., Kang, D. I., Shin, S. Y., Hahm, K-.S., Kim, Y. (2006) Interaction between the plasma membrane and the antimicrobial peptide HP(2-20) and its analogues derived from *Helicobacter Pylori*, *Biochem. J. 394* (1), 105−114.
45. Ghosh, A. K., Rukmini, R., and Chattopadhyay, A. (1997) Modulation of Tryptophan Environment in Membrane-Bound Melittin by Negatively Charged Phospholipids: Implications in Membrane Organization and Function, *Biochemistry 36*, 14291−14305.
46. Avrahami, D., Oren, Z., Shai, Y. (2001) Effect of multiple aliphatic amino acids substitutions on the structure, function, and mode of action of diastereomeric membrane active peptides, *Biochemistry 40* (42), 12591−12603.
47. Shai, Y. (2002) From innate immunity to de-novo designed antimicrobial peptides, *Curr. Pharm. Des. 8* (9), 715−725.
48. Li, X., Li, Y., Han, H., Miller, D. W., Wang, G. (2006) Solution structures of human LL-37 fragments and NMR-based identification of a minimal membrane-targeting antimicrobial and anticancer region, *J. Am. Chem. Soc. 128* (17), 5776−5778.
49. Song, Y. M., Park, Y., Lim, S. S., Yang, S. T., Woo, E. R., Park, I. S., Lee, J. S., Kim, J. I., Hahm, K. S., Kim, Y., Shin, S. Y. (2005) Cell selectivity and mechanism of action of antimicrobial model peptides containing peptoid residues, *Biochemistry 44* (36), 12094−12106.
50. Zhu, W. L., Lan, H., Park, Y., Yang, S. T., Kim, J. I., Park, I. S., You, H. J., Lee, J. S., Park, Y. S., Kim, Y., Hahm, K. S., Shin, S. Y. (2006) Effects of Pro → peptoid residue substitution on cell selectivity and mechanism of antibacterial action of tritrpticin-amide antimicrobial peptide, *Biochemistry 45* (43), 13007−13017.
51. Moon, W. J., Hwang, D. K., Park, E. J., Kim, Y., Chae, Y. K. (2007) Recombinant expression, isotope labeling, refolding, and purification of an antimicrobial peptide, piscidin, *Protein Expression Purif. 51* (2), 141−146.

BI062233U